Benha Journal of Applied Sciences (BJAS) **print: ISSN 2356–9751**
Vol.(5) Issue(7) Part (2) (2020), (217-229) **online: ISSN 2356–976x**
http://bjas.journals.ekb.eg

Sol-Gel Auto-Combustion Synthesis and Identification of Silicon Dioxide Nanoparticles forThe Removal of Sunset Dye from Aqueous Solutions

A. A. Ali, M. Y. Nassar, S. A. Shama, A. M. El Sharkwy, and N. E. El Sayed
Chemistry Department, Faculty of Science, Benha University, Benha, Egypt
E-Mail: Medoohima555@yahoo.com

Abstract

Silica nanoparticles have been successfully synthesized by utilizing sol-gel auto-combustion method using fuels (oxalic acid and citric acid) followed by the calcination at 850 ^{o}C for 4 h. The fabricated silica nanoparticles were characterized by various tools such as X-ray diffraction (XRD), Fourier transform infrared analysis (FT-IR), Field-emission scanning electron microscope (FE-SEM) and high-resolution transmission electron microscope (HR-TEM). The batch adsorption was applied for the removal of sun set dye over the fabricated silicon oxide adsorbent under various experimental conditions. The extracted adsorption data were examined using some adsorption isotherm and kinetic models. The thermodynamic parameters were calculated for the removal of sun set dye over silicon oxide nanoparticles.

Keywords: Silica nanoparticles; Sol-gel auto-combustion method; Organic fuel; Morphology; Calcination

1. Introduction

Metal oxide nanoparticles are required due to its application in electronic, optical, magnetic, chemical catalytic and mechanical properties originating from the high surface to volume ratio, high density of surface sites and quantum size effect [1, 2]. Transition metal oxides (TMO) are the most widely used in the emerging field of magneto-electronics, catalysts, and photo catalysis, solar-cells, and gas- sensors applications [3, 4]. Silicon oxide has many crystalline structures in the form of Quartz, Cristobalite and Tridymite. Besides, the most important form of silicon dioxide is amorphous phase which can be used in different applications. The optical properties having larger transition strengths and index of refraction of crystalline quartz and amorphous silicon oxide [5-7]. Crystalline silicon oxide has more sharp features in the inter-band transition strength spectrum than amorphous silica. The energy of the absorption edge for crystalline SiO_2 is about 1eV higher than that for amorphous one [8, 9]. There are several methods that have been used for the synthesis of silicon oxide nanoparticles as micro-emulsion [1, 10], combustion [11, 12], hydrothermal [13, 14], sol-gel [15-17], etc. There is a significant interest in the synthesis of crystalline and amorphous material for the various applications: microelectronics, optical, electrical, etc. Silica nanoparticles with high purity have a lot of potential applications in many fields such as water treatment, sensor devices and catalysis and dielectric materials [2, 18]. Silicon oxide nanoparticles have been used in the removal of a number of pollutants such as dyes [19, 20], antibiotics [21], heavy metals [22, 23] by adsorption process. The elimination of various dyes from the waste waters of textile industries is also a remarkable field. The hybrid sol–gel auto-combustion synthesis method is used for the preparation of various simple and composite metal oxides [24-29]. In this work, sol-gel auto-combustion method has been used for the synthesis of silica nanoparticles. The composition and morphology of the obtained crystalline silicon

oxide were examined by different equipments including X-ray diffraction, FT-IR analysis, FE-SEM and HR-TEM.

2. Experimental

2.1. Materials and reagents

All chemicals were obtained and used as received without any purification. Sodium metasilicate pentahydrate ($Na_2SiO_3.5H_2O$; 98%) and sun set dye ($C_{16}H_{10}NaO_7S_2$) were obtained from Sigma-Aldrich company. Anhydrous citric acid (CA: $C_6H_8O_7$; 99.5%), oxalic acid (OX: $C_2H_2O_4$), nitric acid (70% HNO_3) and ammonium hydroxide (NH_4OH, 25%) were supplied by El-Nasr Pharmaceutical Chemicals Company.

2.2. Auto-combustion synthesis of SiO_2 nanoparticles

Sodium metasilicate (0.02 mol) was dissolved in 25 ml of distilled water. The pH of the solution was adjusted by addition of HNO_3 (2M) to get pH 9 and the gel was formed. The gel was washed by distilled water and certain amount of the organic fuel (OX, CA and a mixture of them) was added. The obtained mixture was dried at 80 ^oC for 5h followed by auto-ignition at 300 ^oC for few minutes. The obtained ashes were calcined at 500 ^oC for 1h and annealed at 850 ^oC for 4h to obtain white crystalline silicon oxide. Figure 1 presents the flowchart of the fabrication of silicon oxide nanoparticles using sol-gel auto-combustion method using different fuels. Table 1 outlined the products labels, the ratios between the reactants according to the type of fuel in the combustion method. The samples were named as S18, S28 and S38 after calcination at 850 ^oC for 4h

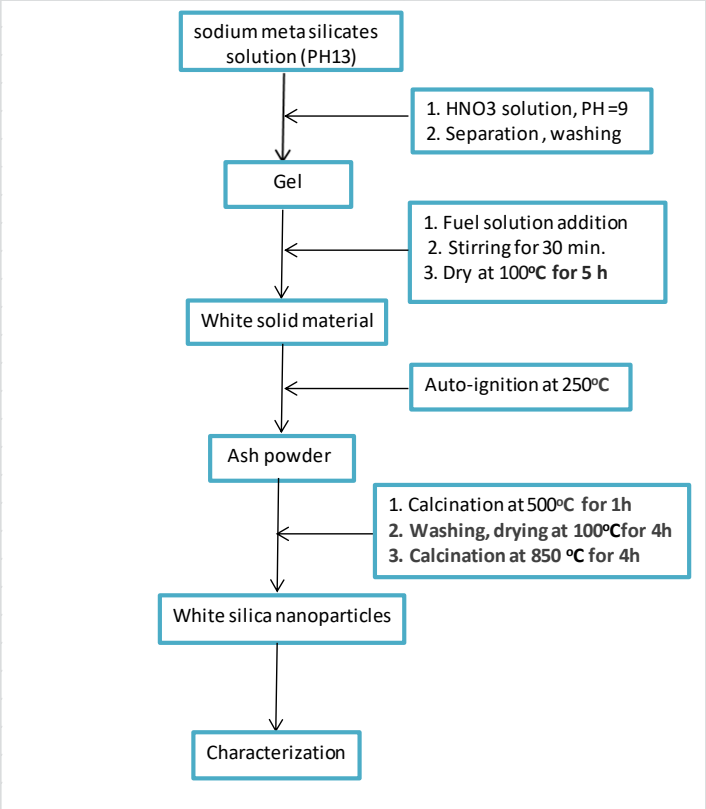

Fig(1) Schematic flowchart for the synthesis of SiO_2 nanoparticles

Table(1) presents the labels of the products and the ratios between the reactants in the preparation of silicon oxide

S. name	Si^{4+}	Organic Fuel			Si^{4+}/ Fuel, molar ratio
		OX	CA	Ox +CA	
S1	0.02	25			1 : 10
S2	0.02		4.7		1 : 1.25
S3	0.02			14.85	1 : 5 : 0.625

3. Characterization

Powder X-ray diffraction (XRD) of the products was measured using diffractometer (Bruker; model D8 advance) with monochromnated Cu-Ka radiation, 1.54178 (˚A) in the 2θ range of 15-80. FT-IR spectra were taken using FT-IR spectrometer (Bomem; model MB 157S) from 4000 to 400 cm^{-1} at room temperature. The morphology and particle size of samples are studied by using Field emission scanning electron microscope (FE-SEM, JEOL: model JSM-6500F) and HR-TEM (model Tecnai G20, FEI, Netherland) at an electron voltage of 200 KV.

3. Results and discussion

3.1. X-ray diffraction (XRD) of SiO_2 nanoparticles

The phase composition and crystallite sizes of the synthesized materials were studied using X-ray analysis and displayed in Fig. 2. XRD patterns of the silicon oxide (S18, S28 and S38 samples) produced by sol-gel auto-combustion method and followed by the calcination at 850 ˚C for 4 h were depicted in Fig. 2. It was observed that the pure crystalline silicon oxide nanoparticles were obtained with the diffraction patterns according to XRD card No. 82-1403 and 86-0681 for cristobalite and tridymite except S18 sample which was amorphous. From the extracted data of XRD analysis, the effect of fuel appeared on the synthesized silicon oxide phase. The average crystallite size (S) of the fabricated silicon oxide was determined from the x-ray diffraction peaks to be 3 nm and 3.5 nm for S28 and S38, respectively.

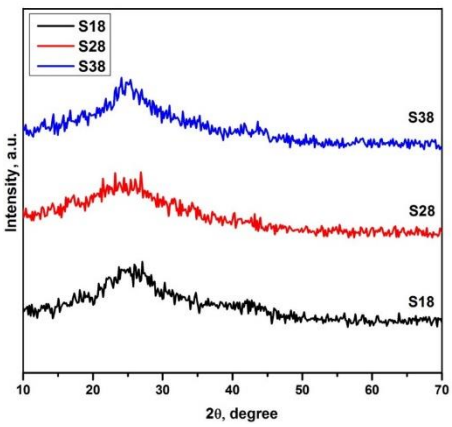

Fig(2) XRD patterns of silica oxide products after calcination at 850 ºC for 4 h

3.2. Fourier transforms infrared analysis (FT-IR)

According to Fig. 3, FT-IR spectra of the as-prepared silicon oxide were recorded in the wavenumber range of 400-4000 cm^{-1}. The weak absorption bands at 3000−3500 cm^{-1} are related to the stretching vibration of hydroxyl groups, originating from organic material and adsorbed water on the surface of the fabricated silicon oxide [30]. The absorption bands at 450, 800 and 1090 cm^{-1} can be assigned to the Si-O band [29]. After calcination, the weak absorption bands in the range 3000-3500 cm^{-1} disappeared which can be assigned to the hydroxide groups and adsorption water over the surface of silicon oxide as shown in Fig.4. The intensity of absorption bands in the range 1100-400 cm^{-1} increased which related to the metal oxide bands. The characteristic absorption bands at 450, 800 and 1090 cm^{-1} are associated to the stretching and bending vibration mode of Si-O bands for S18, S28 and S38 samples [14].

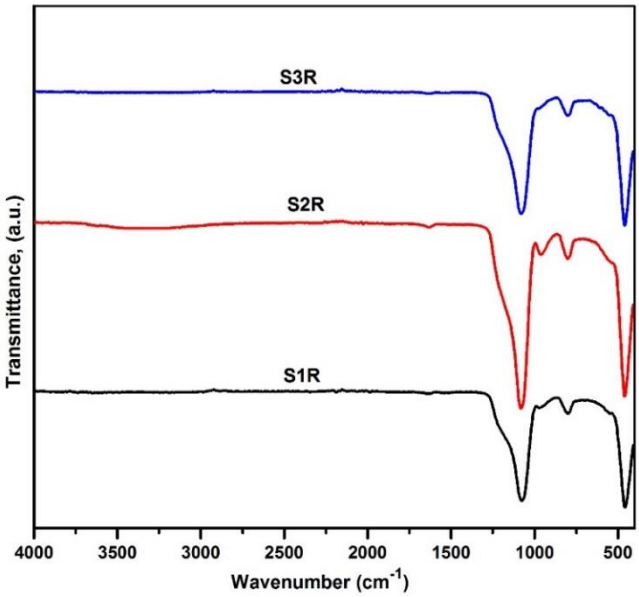

Fig(3) FT-IR spectra of the synthesized silica oxide without calcination (S1R, S2R and S3R samples)

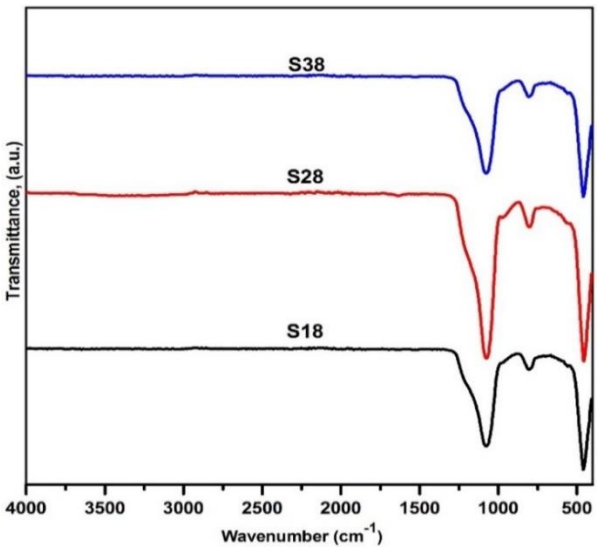

Fig(4) FT-IR spectra of the synthesized silica oxide products after calcination at 850 (S18, S28 and S38 samples)

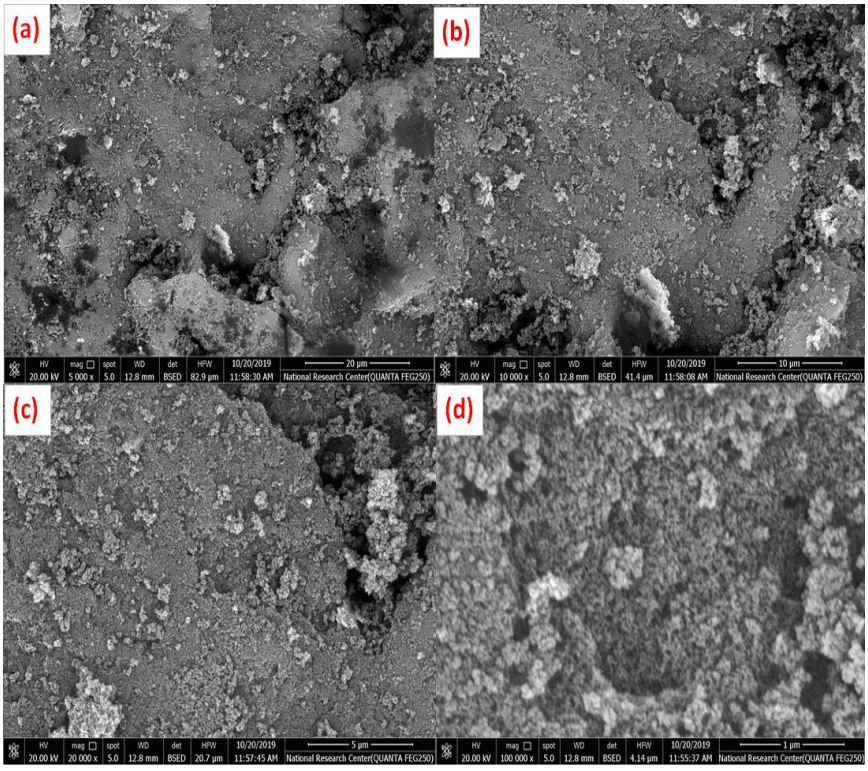

Fig(5) FE-SEM images of silicon oxide nanoparticles (S38 sample) after calcination at 850 ºC for 4 h

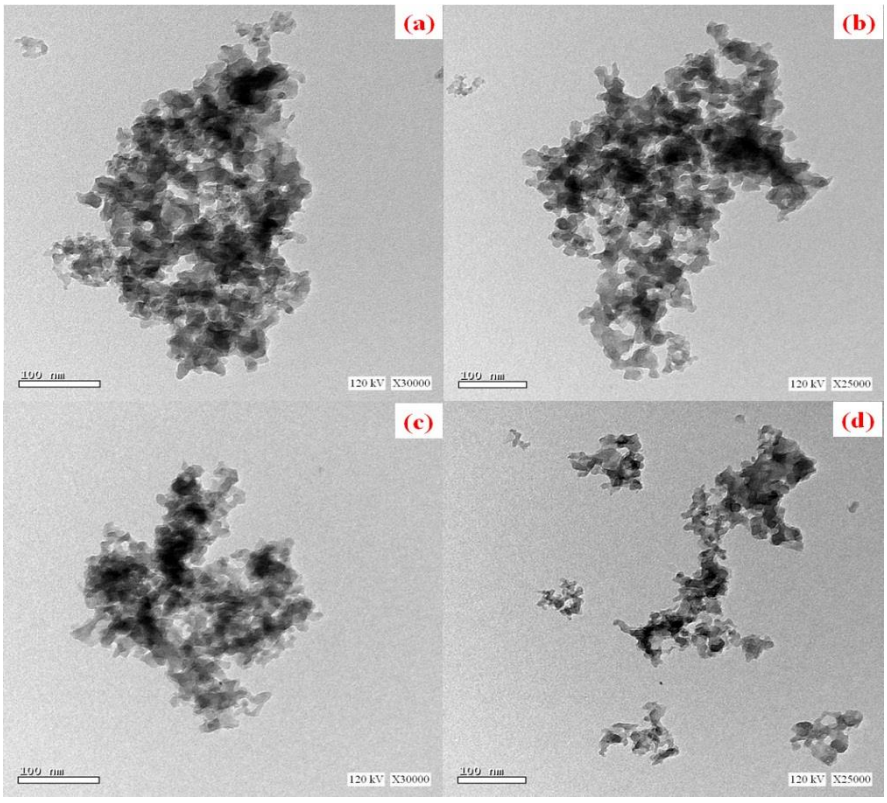

Fig(6) HR-TEM images of silicon oxide nanoparticles (S38 sample) after calcination at 850 ºC for 4 h

3.3 Morphology studies

FE-SEM was used to study the morphology of the calcined SiO_2 at 850 ^oC as represented in Fig. 5(a-d). The FE-SEM micrograph shows an agglomeration of spherical silica oxide nanoparticles. The morphology of the synthesized SiO_2 nanoparticles has been investigated by high-resolution transmission electron microscopy (HRTEM) as shown in Fig. 6(a-d). TEM images display that the silicon oxide nanoparticles are composed of complete and incomplete spherical particles with an average diameter of 16.16 nm.

4. Adsorption studies

The synthesized silicon oxide is used for the adsorption of sun set dye from aqueous media. Different factors that are required for the study of the elimination of sun set dye like pH, adsorbent dose, time and temperature which were studied. The removal of the sun set dye (50 mg/L) over 50 mg of the synthesized silicon oxide was studied over a wide range of pH from 2 to 8 as shown in Fig. 7(a)**.** After stirring for 24 h, the removal efficiency of sun set dye reached its maximum which found to be 12 % (where, λ max =482 nm at pH 2). The contact time of the adsorption of sun set (20 mg/L) was examined at pH 2 and 0.05 g of silicon oxide SiO_2 with stirring for 180 min. The removal efficiency of sunset dye was rapidly increased and recorded 26 % at 60 min. The equilibrium condition was attained in between 100-180 min and the removal percentage was found to be 28 %. The removal of sun set dye was examined by using 50 mg of SiO_2 nanoparticles at pH 2 and the initial concentrations were used in range of 10 - 50 mg/L. After 140 min of stirring, the adsorption capacity increased as displayed in Fig. 7(b). 10-100 mg of silicon oxide was examined for the removal of sun set dye of 25 mg/L initial concentration at pH 2. The removal of sun set dye was plotted against the adsorbent does as shown in Fig. 7(c). The extracted data appeared that the removal of dye decreased with raising the amount of silicon oxide. The adsorption studies were carried out at 30, 40 and 50 ^oC, separately and the selected conditions were pH 2, 25 mg/L and 140 min contact time. The experimental study revealed that the removal decreased slowly by increasing temperature as shown in Fig. 7(d). Based on the obtained data, we can conclude that the adsorption of sun set was an exothermic process.

5. Adsorption isotherms

Langmuir and Freundlich isotherm models were tested using 50 mg of silicon oxide and the determined experimental data as the following: 10-50 mg/L, pH 2, 30 ^oC and 140 min. the selected isotherm models were applied for an adsorption data using the following equations:

$$C_e/q_e = 1/(q_m\mathrm{B}) + C_e/q_m \quad (1)$$

$$\ln q_e = \ln K_f + \left(\frac{1}{\mathrm{n}}\right)\ln C_e \quad (2)$$

Where C_e, q_e and q_m are the equilibrium concentration of dye (mg/L), amount of adsorbed dye at equilibrium and the maximum capacity of adsorbed dye over silicon oxide (mg/g), respectively. B, K_f and 1/n are Langmuir constant (L/mg), Frendlich constant (mg/g) and the heterogeneity factor, respectively.

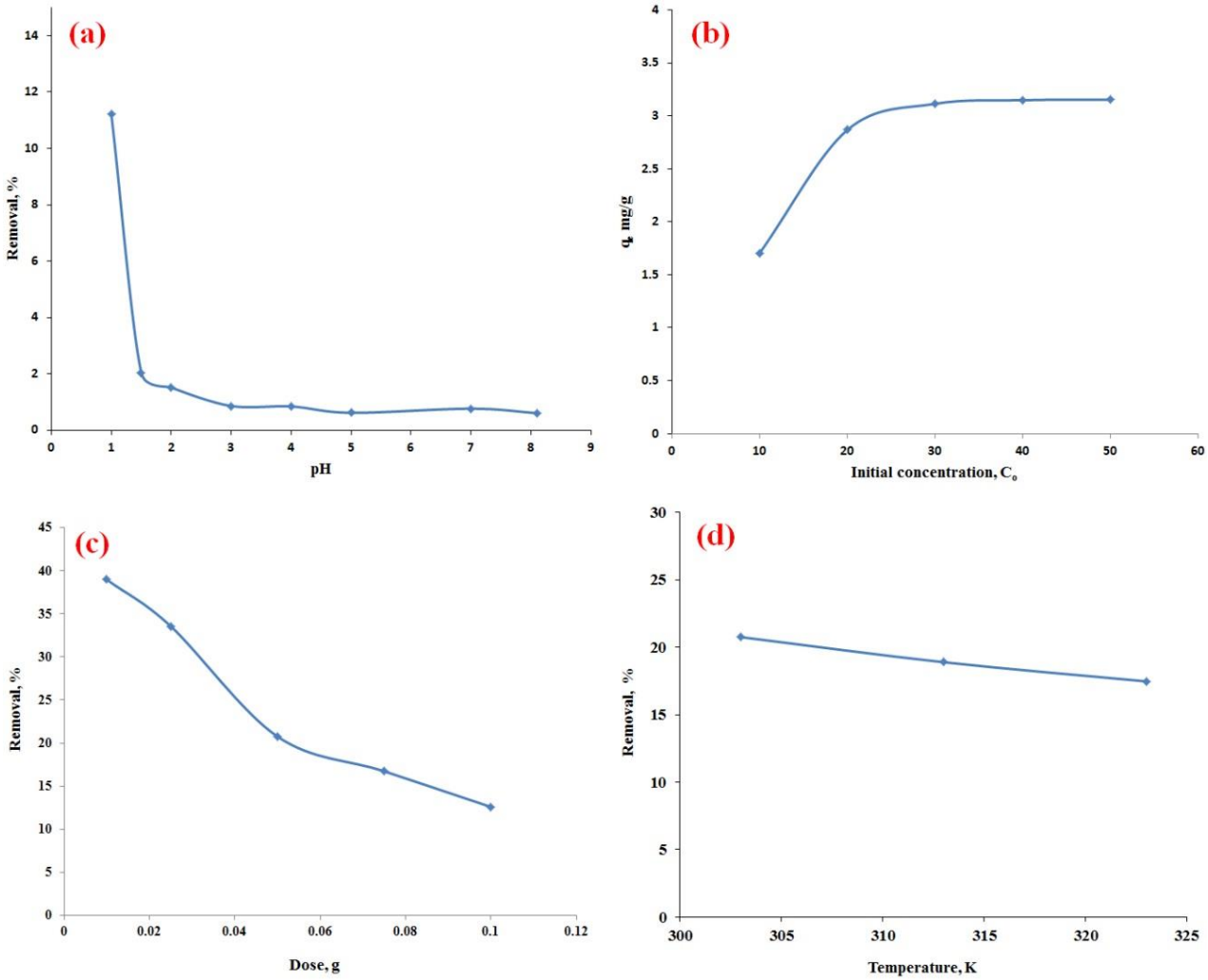

Fig(7) the study of experimental adsorption parameters for the removal of sun set dye over silicon oxide nanoparticles: (a) effect of pH, (b) effect of initial concentration, (c) effect of dose and (d) effect of temperature

Fig(8) displayed Langmuir and Freundlich isotherm models for the removal of sun set dye over silicon oxide nanoparticles. Table 2 are outlined the extracted factors from Langmuir and Freundlich isotherm. From the R^2 values, Langmuir isotherm model was a better fitting than the Freundlich isotherm. Besides, the estimated adsorption capacity from Langmuir isotherm was estimated to be 3.62 mg/g, which were consistent with the experimental value (3.11 mg/g). From Table (2), R_L values show that the adsorption of sun set dye over silicon oxide nanoparticles was a favorable process.

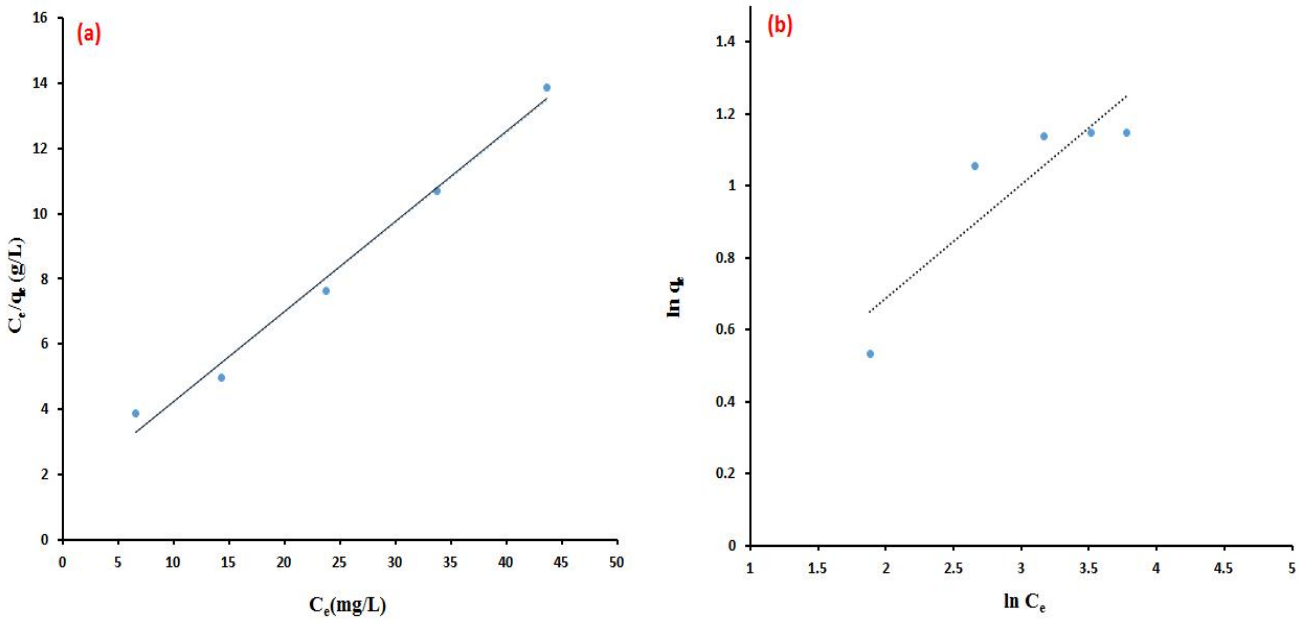

Fig(8) Langmuir (a) and Freundlich (b) isotherm models for the removal of sun set dye over silicon oxide nanoparticles

Table(2) The extracted parameters from the isotherms for the removal of sun set dye on silicon oxide nanoparticles

Adsorption isotherm	Parameter	SiO_2
Langmuir parameters	K_L (L/mg)	0.18793
	$q_{m\,(cal)}$ (mg/g)	3.622
	R_L	0.09619 - 0.34731
	R^2	0.9884
	$q_{m\,(exp)}$ (mg/g)	3.11
Freundlich parameters	K_F [(L/mg) (L/mg)$^{1/B}$]	1.0543
	$q_{m\,(cal)}$ (mg/g)	2.723
	B	3.158
	R^2	0.8028
	$q_{m\,(exp)}$ (mg/g)	3.11

6. Kinetic studies

Pseudo first and pseudo second order reaction models were used for investigation of the rate of the remove of sun set dye over the fabricated silicon oxide by utilizing the following equations:

$$\log(q_e - q_t) = \log q_e - \frac{K_1}{2.303}\, t \quad (3)$$

$$\frac{t}{q_t} = \frac{1}{K_2 q_e{}^2} + \frac{t}{q_e} \quad (4)$$

Where, q_e and q_t are the quantities of adsorbed dye (mg/g) at time and equilibrium. K_1 (min^{-1}) and k_2 (g/mg/min) are constants of pseudo-first and pseudo-second-order. Kinetic parameters were listed in Table 3 for the adsorption of sun set dye over the synthesized silicon oxide adsorbent.

According to the correlation coefficients, pseudo second order was acceptable compared to the pseudo first order kinetic models. Depending on the extracted data, the adsorption capacity value (3.15 mg/g) calculated from pseudo-second-order kinetic model was close to the experimental value (2.87 mg/g) for the removal of sunset dye over silicon oxide adsorbent. These results suggested that the pseudo second-order can be applied. Kinetic model could describe the obtained adsorption data.

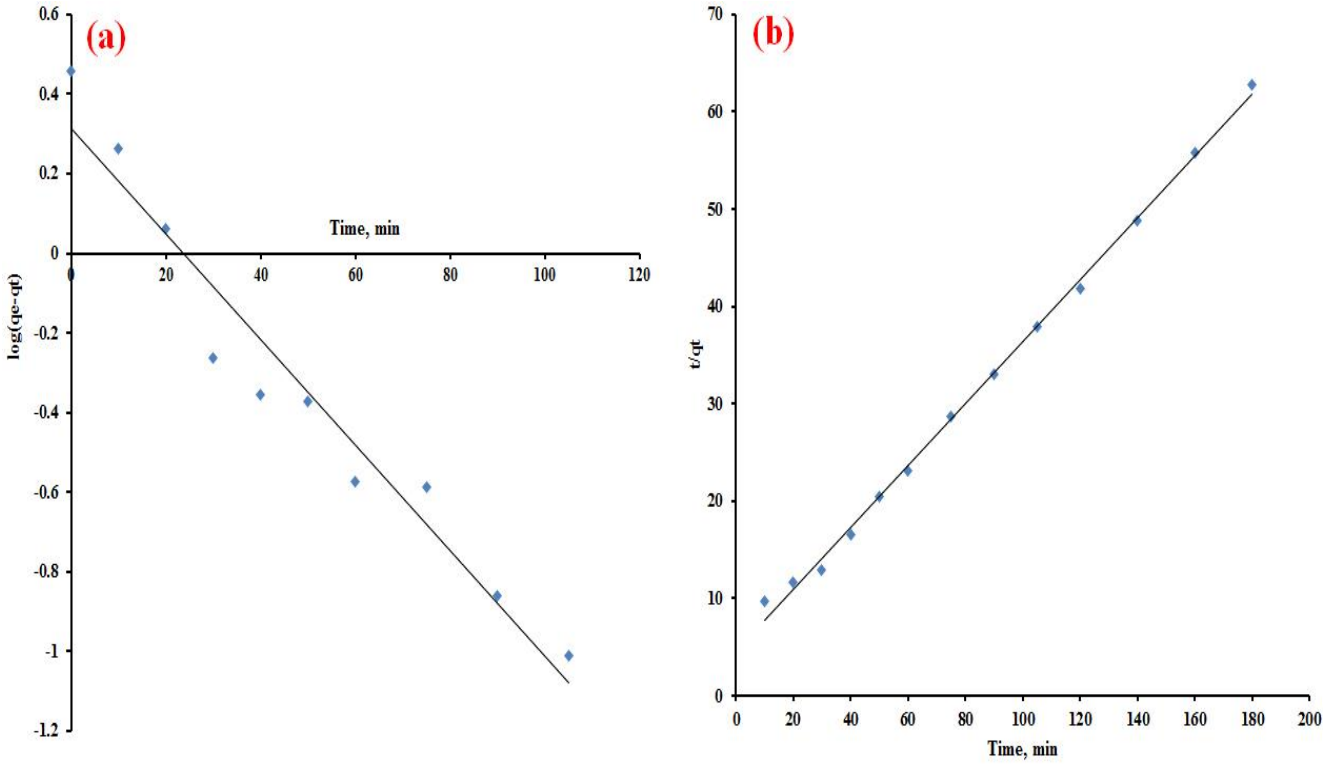

Fig(9) Pseudo first order model (a), Pseudo second order model (b), for removal the sunset dye using silicon oxide sample

Table(3)Kinetic parameters for adsorption of sun set dye over the synthesized silicon oxide adsorbent

Kinetic model	Parameter	SiO_2
Pseudo first order	$K_1(min^{-1})$	0.071854
	$q_{m\,(cal)}$ (mg/g)	2.054471
	R^2	0.9287
	$q_{m\,(exp)}$ (mg/g)	2.87
Pseudo second order	K_2 (g/mg.min)	0. 021849
	$q_{m\,(cal)}$ (mg/g)	3.147624
	R^2	0.9849
	$q_{m\,(exp)}$ (mg/g)	2.87

7. Thermodynamic studies

Thermodynamic parameters (entropy change (ΔS^o), enthalpy change (ΔH^o), and free energy change (ΔG^o) were estimated for the adsorption data using the following:

$$\ln K_d = \frac{\Delta S^\circ}{R} - \frac{\Delta H^\circ}{RT} \quad (5)$$

$$\Delta G^\circ = \Delta H^\circ - T\Delta S^\circ \quad (6)$$

$$K_d = q_e/C_e \quad (7)$$

Where K_d is the Equilibrium constant, q_e is the adsorbent equilibrium concentration (mg/L), T in Kelvin and R is the observed gas constant. Plotting ln K_d against 1/T gives a straight line with slope and intercept equal to [$-\Delta H^o/R$] and [$\Delta S^o/R$], respectively. Thermodynamic parameters are determined and listed in Table 4.

The removal of sun set dye using silicon oxide nanoparticles were exothermic process. Since the value of ΔH^o was lower than 40 KJ/mol, the adsorption of sun set dye using silicon oxide is the physisorptive process. ΔS^o has negative charge which means decreasing in degree of freedom of solution for removal sun set dye using silicon oxide. The positive values of ΔG^o revealed that the separation process was a nonspontaneous process. Additionally, the increasing of ΔG^o values with the raising of temperature shows that the adsorption of sun set dye using silicon oxide is unfavorable at high temperatures.

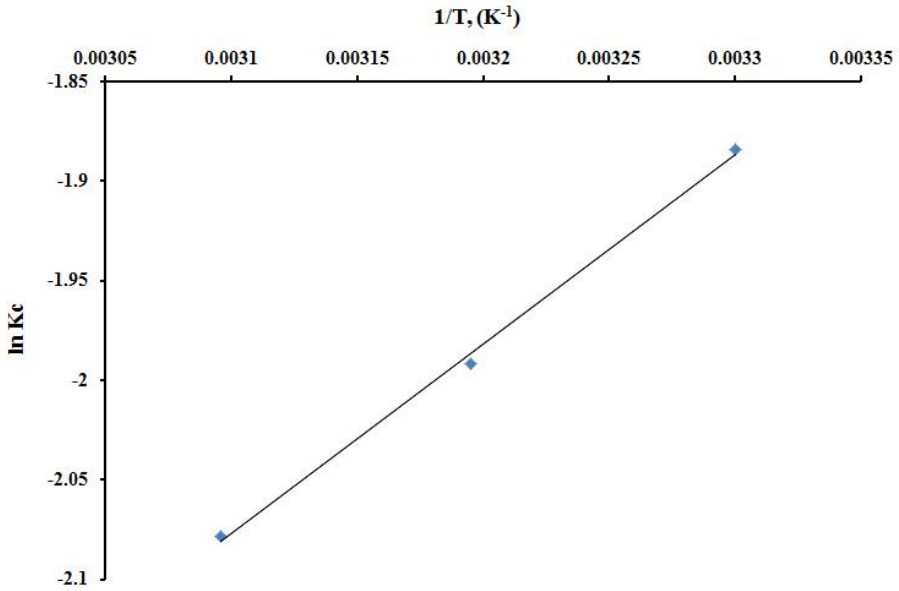

Fig(10) Vant Hoff plot for the adsorption of sun set dye on silicon oxide nanoparticles

Table(4)Thermodynamic data for adsorption of sun set dye over the synthesized silicon oxide adsorbent

Sample	T, (ºK)	ln K_c	ΔGº (KJ/mol)	ΔHº (KJ/mol)	ΔSº (KJ/mol)
S8	303	-1.88433	4.753	- 7.89	- 0.04174
	313	-1.99165	13.06		
	323	-2.07819	13.48		

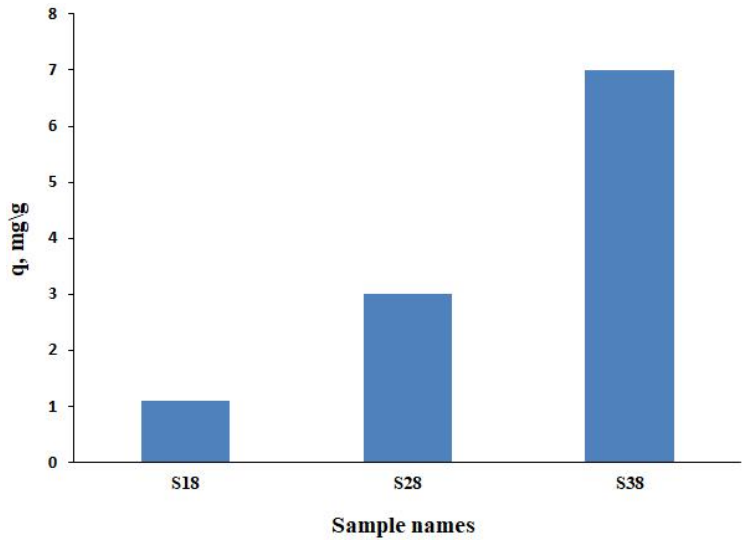

Fig(11) The adsorption capacities of the synthesized adsorbents (S18, S28 and S38) after applied the optimum conditions

8. Effect of the used fuel on the adsorption capacities of the synthesized adsorbents

The adsorption capacities of the as-prepared adsorbents using via the sol-gel auto combustion method using (oxalic, citric acid and mixed of them) fuels. The obtained samples (S18, S28 and S38) were studied at pH=2, 25 mg/L of sun set dye, 0.025 g dose adsorbents and equilibrium time 140 min. The adsorption capacities of SiO_2 nanoparticles are determined as displayed in Figure 11.

5. Conclusions

SiO_2 nanoparticles were synthesized by sol-gel auto-combustion method using sodium metasilicate and fuels. The obtained samples were characterized by using various tools. XRD patterns of the synthesized samples showed the characteristic peaks of silicon oxide. The specific absorption peaks at at 450, 800 and 1090 cm^{-1} are associated to the stretching and bending vibration mode of Si-O inside SiO_2. The FE-SEM photograph displayed the calcined SiO_2 has spherical shape and the average size of particles in range of 1µm. The TEM photographs displayed that the calculated average particle size was about 16.16 nm. It was found that the rate of adsorption of sun set dye obeyed the pseudo-second-order kinetic model. The adsorption process of sun set dye over SiO_2 nanoparticles fitted Langmuir isotherm model. The calculated thermodynamic factors (ΔG^o, ΔH^o and ΔS) exhibited that the adsorption process of sun set dye on silicon oxide was exothermic, physisorptive, nonspontaneous and unfavorable at high temperatures.

Acknowledgements

The authors express their thanks to Benha University, Egypt for support of the current research.

References

[1] H. Azlina, J. Hasnidawani, H. Norita, S. Surip, Synthesis of SiO_2 nanostructures using sol-gel method, Acta Phys Pol A, Vol.(129), PP.842-844, 2016.

[2] R. Dubey, Y. Rajesh, M. More, Synthesis and characterization of SiO2 nanoparticles via sol-gel method for industrial applications, Materials Today: Proceedings, Vol.(2), PP.3575-3579, 2015.

[3] M.Y. Nassar, T.Y. Mohamed, I.S. Ahmed, I. Samir, MgO nanostructure via a sol-gel combustion synthesis method using different fuels: an efficient nano-adsorbent for the removal of some anionic textile dyes, Journal of Molecular Liquids, Vol.(225), PP.730-740, 2017.

[4] M.Y. Nassar, A.A. Ali, A.S. Amin, Correction: A facile Pechini sol–gel synthesis of TiO2/Zn2TiO2/ZnO/C nanocomposite: an efficient catalyst for the photocatalytic degradation of Orange G textile dye, RSC Advances, Vol.(7), PP.33257-33257, 2017.

[5] E. Suzuki, High-resolution scanning electron microscopy of immunogold-labelled cells by the use of thin plasma coating of osmium, Journal of microscopy, Vol.(208), PP.153-157, 2002.

[6] R.F. Lenza, W.L. Vasconcelos, Preparation of silica by sol-gel method using formamide, Materials Research, Vol.(4), PP.189-194, 2001.

[7] V. Henrich, P. Cox, The surface chemistry of metal oxides, in, Cambridge University Press, Cambridge, UK, 1994.

[8] M. Valden, X. Lai, D.W. Goodman, Onset of catalytic activity of gold clusters on titania with the appearance of nonmetallic properties, science, Vol.(281), PP.1647-1650, 1998.

[9] R. Nandanwar, P. Singh, F.Z. Haque, Synthesis and characterization of SiO2 nanoparticles by sol-gel process and its degradation of methylene blue, Am. Chem. Sci. J, Vol.(5), PP.1-10, 2015.

[10] A. Tavakoli, M. Sohrabi, A. Kargari, A review of methods for synthesis of nanostructured metals with emphasis on iron

compounds, Chemical Papers, Vol.(61), PP.151-170, 2007.
[11] A. Ali, E. El Fadaly, I. Ahmed, Near-infrared reflecting blue inorganic nano-pigment based on cobalt aluminate spinel via combustion synthesis method, Dyes and Pigments, Vol.(158), PP.451-462, 2018.
[12] Y. Ni, X. Cao, G. Wu, G. Hu, Z. Yang, X. Wei, Preparation, characterization and property study of zinc oxide nanoparticles via a simple solution-combusting method, Nanotechnology, Vol.(18), PP.155603, 2007.
[13] S. Bazazi, N. Arsalani, A. Khataee, A.G. Tabrizi, Comparison of ball milling-hydrothermal and hydrothermal methods for synthesis of ZnO nanostructures and evaluation of their photocatalytic performance, Journal of Industrial and Engineering Chemistry, Vol.(62), PP.265-272, 2018.
[14] M.N. Núñez, A. Martínez-de la Cruz, Nitric oxide removal by action of ZnO photocatalyst hydrothermally synthesized in presence of EDTA, Materials Science in Semiconductor Processing, Vol.(81), PP.94-101, 2018.
[15] R. Bekkari, D. Boyer, R. Mahiou, B. Jaber, Influence of the sol gel synthesis parameters on the photoluminescence properties of ZnO nanoparticles, Materials Science in Semiconductor Processing, Vol.(71), PP.181-187, 2017.
[16] A.K. Zak, M.E. Abrishami, W. Abd, Majid, Ramin Yousefi, SM Hosseini, Ceram Int, Vol.(37), PP.393-398, 2011.
[17] I.A. Rahman, V. Padavettan, Synthesis of silica nanoparticles by sol-gel: size-dependent properties, surface modification, and applications in silica-polymer nanocomposites—a review, Journal of Nanomaterials, PP.8, 2012.
[18] A.Y. Arasi, M. Hemma, P. Tamilselvi, R. Anbarasan, Synthesis and characterization of SiO2 nanoparticles by sol-gel process, Indian Journal of Science, Vol.(1), PP.6-10, 2012.
[19] R.D. Kale, P.B. Kane, Colour removal using nanoparticles, Textiles and Clothing Sustainability, Vol(2), PP.4, 2017.
[20] Z. Wang, C. Yu, C. Fang, M. Mallavarapu, Dye removal using iron–polyphenol complex nanoparticles synthesized by plant leaves, Environmental Technology & Innovation, Vol.(1), PP.29-34, 2014.
[21] D. Balarak, Y. Mahdavi, F.K. Mostafapour, Application of alumina-coated carbon nanotubes in removal of tetracycline from aqueous solution, Journal of Pharmaceutical Research International, PP.1-11, 2016.
[22] S. Mahdavi, A. Afkhami, H. Merrikhpour, Modified ZnO nanoparticles with new modifiers for the removal of heavy metals in water, Clean Technologies and Environmental Policy,Vol.(17), PP.1645-1661, 2015.
[23] A. Ahmadi, S. Heidarzadeh, A.R. Mokhtari, E. Darezereshki, H.A. Harouni, Optimization of heavy metal removal from aqueous solutions by maghemite (γ-Fe2O3) nanoparticles using response surface methodology, Journal of Geochemical Exploration, Vol.(147), PP.151-158, 2014.
[24] H.C. Yi, J.J. Moore, Self-propagating high-temperature (combustion) synthesis (SHS) of powder-compacted materials, Journal of Materials Science, Vol.(25), PP.1159-1168, 1990.
[25] K. Patil, M. Hegde, T. Rattan, S. Aruna, Chemistry of Combustion Synthesis, Properties and Applications Nanocrystalline Oxide Materials, World Scientific Publishing Co. Pte. Ltd., Singapore, 2008.
[26] A.S. Mukasyan, P. Epstein, P. Dinka, Solution combustion synthesis of nanomaterials, Proceedings of the combustion institute, Vol.(31), PP.1789-1795, 2007.
[27] I. Ahmed, H. Dessouki, A. Ali, Synthesis and characterization of new nano-particles as blue ceramic pigment, Spectrochimica Acta Part A: Molecular and Biomolecular Spectroscopy, Vol.(71), PP.616-620, 2008.
[28] A.A. Ali, E. El Fadaly, I.S. Ahmed, Near-infrared reflecting blue inorganic nano-pigment based on cobalt aluminate spinel via combustion synthesis method, Dyes and Pigments, Vol.(158), PP.451-462, 2018.
[29] A.A. Ali, M.R. Allazov, T.M. Ilyasli, Synthesis and characterization of magnesium aluminates spinel via combustion method using malonic acid dihydrazide as fuel, Caspian Journal of Applied Sciences Research,Vol.(2), PP.85-90, 2013.
[30] H.V. Vasei, S. Masoudpanah, M. Adeli, M. Aboutalebi, Solution combustion synthesis of ZnO powders using CTAB as fuel, Ceramics International, Vol.(44), PP.7741-7745, 2018.